



Prediction of Tool Force in Two Point Incremental Forming by Slab Analysis

M. Esmailian, K. Khalili*

Department of Mechanical Engineering, University of Birjand, Birjand, Iran

PAPER INFO

Paper history:

Received 30 June 2020

Received in revised form 26 August 2020

Accepted 03 September 2020

Keywords:

Two Point Incremental Forming

Tool Force

Slab Analysis

CNC Machine

ABSTRACT

Two-Point Incremental Forming (TPIF) method is a novel technique for producing free form shell parts. The main purpose of this study is to analyze the TPIF process, and, by approximate calculation, to find the force applied to the tool. One of the limitations of an incremental forming process is that during this process force applied to the tool is born by the machine. In this research, an equation for approximate prediction of the force applied to the tool is presented using the values of the yield stress of the sheet, friction coefficient, tool radius and thickness of the sheet; hence, the applied force can be calculated. By increasing the forming angle, the amount of the created local strain increases and the change in thickness and the force applied to the tool is enhanced. However, by increasing the angle of punch wall, less compressive stress is applied to the metal sheet due to the reduction in contact between the surface of the tool and punch wall. Analytical equations presented are validated by the results from experimental tests.

doi: 10.5829/ije.2020.33.11b.30

1. INTRODUCTION

Producing parts from metal sheets by using molds and special tools is not economical in research and development or in some industries, such as aerospace, where production circulation is low. Hence, using the incremental forming method is one of the best choices. To form parts, in addition to axial symmetric forms, some incremental forming methods, such as Single Point Incremental Forming (SPIF), in which the motion of the tool is guided by a Computer Numerical Control (CNC) machine, have been developed.

According to Figure 1, in this process, a small spherical-head tool that has a single-point contact with the sheet moves in a specific direction by the user and creates the final form on the sheet [1]. This process was first presented by Edward [2]. However, the main development of this method happened with the advent of CNC in the end of 1970s. In this period, Mason and Appleton [3] introduced the asymmetric incremental forming for the first time and indicated that, using CNC, the formability of a metal sheet is possible as a spherical-head tool moves on it. The main advantages of

incremental forming method are: 1) the low cost of this method compared to other conventional forming methods [4]; 2) high formability due to the possibility of changing the form of the final part by changing the CNC program [5]; 3) higher formability of the sheet compared to other methods because of applying force to points; and 4) high flexibility/simple set up in rapid prototyping, or when mass production is not an aim and ease of selecting the proper machine with less limitations due to the demand for lower forces [6].

Another type of incremental forming method is Two Point Incremental Forming (TPIF), in which a constant punch is placed at the bottom of the sheet, and a spherical-head tool incrementally places the sheet on the punch and the sheet is formed to the form of the bottom punch (Figure 2) [7]. The main difference between the two methods is the higher formability of the sheet.

Different parameters of the incremental forming process are investigated and analyzed by researchers. For instance, by using theories and simulations, different efficient parameters such as temperature [8-10], the maximum angle of the wall [11-13], the vertical pitch of tools [14-16], tool size [15-17] and the direction of the

*Corresponding Author Institutional Email: kkhalili@birjand.ac.ir (K. Khalili)

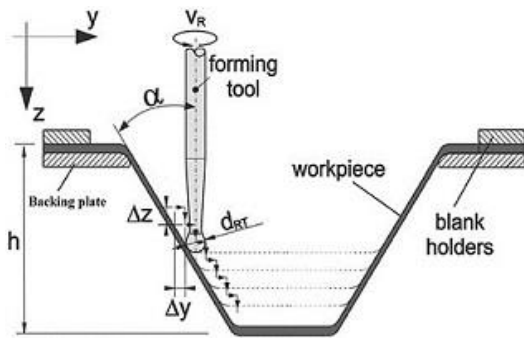


Figure 1. Basic principles of Single Point Incremental Forming [6]

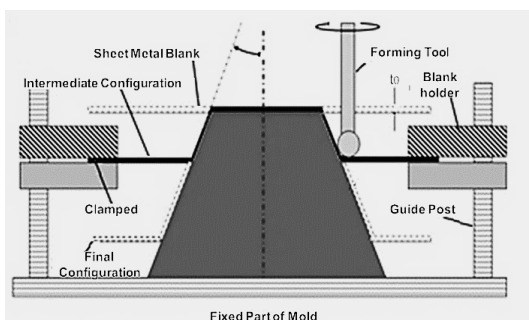


Figure 2. Basic principles of Two Point Incremental Forming [7]

tool [18-19] on the formability of the sheet are investigated. For example, by increasing temperature, decreasing vertical pitch and tool radius, the formability of sheet increases. Other studies have investigated failure and tearing modes of the sheet and parameters effective in the incremental forming process by using experimental methods, theories and simulations.

By investigating the formability of an annealed aluminum sheet in SPIF, Shim and Park [20] declared that the obtained forming limit graph is different from other conventional methods and it is similar to a direct line or a line with negative inclination. Kim and Park [21] studied the effect of process parameters on the formability of an annealed aluminum sheet in SPIF and indicated that, in this process, the formability of sheets is higher than other forming methods. In addition, by using experimental analysis and finite element analysis, they investigated the effect of process parameters, such as size and type of tool, processing rate and friction on the contact surface between the tool and sheet on incremental forming. Moreover, they figured out that by increasing processing rate and decreasing friction, the formability of the sheet is enhanced. Hirt et al. [22] studied two main limitations of the incremental forming process including the available maximum wall angle and the creation of geometrical deviation. They suggested several forming strategies and finite element modeling for incremental forming of the sheet for eliminating the limitations of this

process. Fan et al. [9] presented a method for examining the thinning limit of aluminum sheet by using a truncated cone with the variable angle of the wall. They used a circular arc for modeling a cone wall with variable angles. Silva et al. [23] experimentally studied the fracture mechanism in SPIF for an AA1050-H111 aluminum sheet. In this investigation, the truncated pyramid and cone parts, both with variable angle of the wall, were presented by using different tool diameters. Their results revealed that, by using tools with diameters less than 10 mm, local necking does not occur before fracture. By simulating finite element of incremental forming of a truncated pyramid and extracting forming limit graphs based on stress, Seong et al. [24] proved that the main minimum and maximum stresses are changed along sheet thickness causing the elimination of necking phenomena in SPIF process and, consequently, the enhancement of formability. Kura et al. [25] numerically and experimentally investigated the formability of an extra-tensile steel sheet in SPIF. In the above-mentioned research, a cone with variable wall angles consisting of circular, parabolic and oval was used. The average value of the maximum angle of the wall in the mentioned research was 75.27° .

Oraon and Sharma [26] used an artificial neural network to predict the minimum force required for single point incremental forming (SPIF) of thin sheets of Aluminium AA3003-O and calamine brass Cu67Zn33 alloy. Accordingly, the parameters for processing, i.e., step depth, the feed rate of the tool, spindle speed, wall angle, thickness of metal sheets and type of material were selected as input and the minimum vertical force component was selected as the model output.

Silva et al. [27] provided a new theoretical model for rotational symmetric SPIF that was developed under membrane analysis with bi-directional in-plane contact friction forces. As shown in Figure 3, they divided the formed parts surface into three areas: smooth surface area under surficial and tensile strain (A), rotational symmetric surface under surficial and tensile strain (B) and the angle under the condition of equal tension with two axes (C). Then, they presented a series of analytical

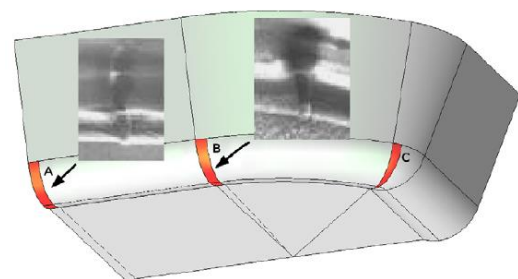


Figure 3. Instantaneous deformation zone and contact between forming tool and workpiece during SPIF [27]

equations for stress and strain values in SPIF. The analytical solutions had some simplifications (they considered the material as rigid, completely plastic and isotropic).

In another work, Silva and Martins [28] proposed a new level of understanding of two-point incremental forming (TPIF) with a partial die using a combined theoretical and experimental investigation. The theoretical developments include an innovative extension of the analytical model for rotational symmetric single point incremental forming (SPIF), originally developed by the authors, to address the influence of the major operating parameters on TPIF and to successfully explain the differences between SPIF and TPIF in formability.

By reviewing previous studies, it can be understood that most of the studies have investigated different aspects of SPIF, and the effect of efficient parameters of TPIF has not been theoretically considered in simulations [29-31]. In the incremental forming process of metal sheets, plastic deformation is considered in a small region of the sheet. Hence, to investigate the theoretical principles governing this process, stress values in this small region should be calculated. Moreover, to analyze this process, the incremental forming process and small deformation area should be considered. Due to the small forming area, the type of punch used at the bottom of the sheet is not important in analytical calculations. The form of punch is determined based on the final form of the product.

The main purpose of this study is an analytical solution for TPIF, and three important objectives are considered in this regard. After approximate calculation of the stress domain, the force applied to the tool can be determined. Approximate calculation of the force on the tool and its prediction before the process are highly important. The force applied to the spindle of CNC has special limitations; therefore, calculation of the force applied to the tool is an appropriate criterion for selecting the type of CNC. In addition, to select the material and size of the tool, the calculated force in this analysis can be used. Moreover, by investigating the force applied during the process, the critical points of TPIF and related conditions are determined. By analyzing this process through the slab method, some parameters such as tool radius, sheet thickness, friction coefficient and punch angle are calculated. Therefore, by calculating the stress domain based on these parameters, the effects of these parameters are investigated. The extracted analytical equations in this study are validated with the results obtained from experimental researches.

2. SLAB METHOD ANALYSIS

In TPIF, when the flat surface of a strained sheet is placed on the punch, the required deformation is created in the

metal sheet; hence, by moving on a specific profile (according to the punch form), a forming tool should perform straining operation on the flat sheet and place it on the punch. This process happens in a very short time by moving the tool on a specific point, and after crossing the tool, similar operations happens in other points of the sheet.

In the forming process, by using conical and multi-dimensional punches (Figure 4), the inclination of the punch wall remains constant and all the points on the sheet surface are strained to the angle α . Therefore, the sheet forming mechanism in different points is theoretically similar, and the values of the created stress and forces in the process remain unchanged.

Theoretical analysis of TPIF is carried on in a region where plastic deformation occurs. In this small region, a part of the spherical-head tool is in contact with the metal sheet. The contact of the tool with the metal sheet and consequently, the amount of applied force from tool to the sheet has a direct relationship with the angle of the punch wall. According to Figure 5, the spherical-head tool is tangent to the sheet surface from point A to point B. Hence, only this part of the tool (AB arc) performs the forming operation. The angle corresponding to this arc equals the angle of the punch wall to horizon (α). The distance of point A equals the vertical axis of the tool ($R_{\text{tool}}\sin\alpha$).

To analyze the incremental forming process, the slab method is used to select an element from the metal sheet on which the forming process is completely concentrated.

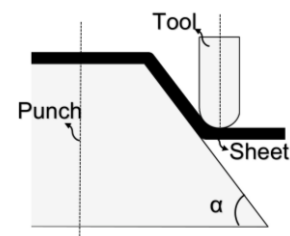


Figure 4. Forming process using conical punch

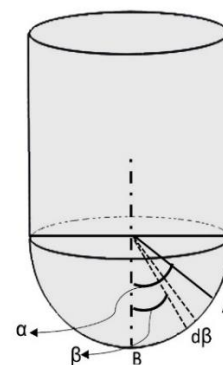


Figure 5. The range of contact of tool and sheet

As shown in Figure 5, this element is a part of the metal sheet placed along AB (contact area between the tool and sheet) at a distance of r from the horizontal axis of the tool. If β is the selected angle element with the vertical axis, the value of r changes from 0 to $R_{tool}\sin\alpha$. Moreover, the relationship between β and r is defined by Equation (1):

$$r = R_{tool}\sin\beta \tag{1}$$

In the calculations presented in this section, the sheet surface is inclined by the angle α and is placed on the punch. These equations are independent of the form of the punch and are usable for all TPIF processes.

In Figure 6, the applied loadings on an element of material are illustrated. This element is a small part of the metal sheet placed on AB arc at a distance of r from the vertical axis of the tool. The thickness of the top face of the element equals $t+dt$ and that of its bottom face equals t . Therefore, the change of sheet thickness in this small region is considered in calculations. As seen in Figure 6, three stress parameters in three orthogonal directions cause the application of force to different faces of the element. Along peripheral direction, the stress σ_θ is applied to two lateral faces of the element. In vertical direction (tangential direction on the tool surface), the stress parameter σ_γ , in addition to straining the smooth surface of the sheet and placing the sheet on the punch, cause the stretching of the sheet along this direction. In addition, the vertical stress applied by the tool to the sheet is denoted by σ_n . To extract balance equations, TPIF process is considered as a quasi-static process. Therefore,

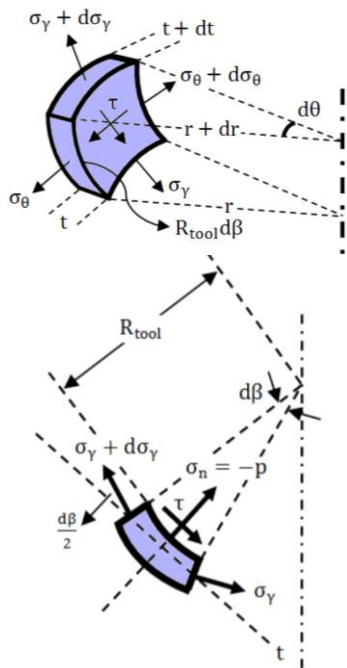


Figure 6. Stress components on the element

by using this method, an initial estimation of the created stress in the material and the required forces during the process are calculated.

In order to use Slab Method analysis, some assumptions are considered for simplifying the extraction of final equations. In these assumptions, the sheet used in forming process is considered an isotropic material, and the changes of yield stress during forming process and creation of rigidity in plastic area are neglected. Therefore, yield stress is considered a constant coefficient (Y).

As mentioned before, friction between the tool and sheet and contact between the sheet and punch create a shear stress on the sheet, which is considered in equations. However, because of its small value, the tensile and compressive stresses applied to the element are considered as the principal stresses. Therefore, to use equations in the plastic region, shear stress is ignored, and its effect is only considered in balance equations. In the presented slab method analysis, the extraction of exact equations is not considered; however, approximate calculation of the values of the stress and forces created during the process is important as an appropriate criterion for the tools and equipment required for the user. According to Figure (6), the balance equation along γ is defined as follows:

$$(\sigma_\gamma + d\sigma_\gamma)(r + dr)(t + dt)d\theta - \sigma_\gamma trd\theta - \tau R_{tool}d\beta rd\theta = 0 \tag{2}$$

In this analysis, the amount of normal stress (the compressive stress applied to the element) is equal to σ_n . Since the numerical value of this parameter is negative, positive P ($P=-\sigma_n$) is used. Therefore, by considering slip friction, shear stress among surfaces is obtained using Equation (3):

$$\tau = \mu p \tag{3}$$

Due to the small value of μp compared to shear yield stress ($Y/\sqrt{3}$), using this assumption is logical. It should be noted that the friction coefficient among surfaces (μ) is selected so that the effect of friction between the tool and sheet, and friction between the sheet and punch are simultaneously considered in calculations. Therefore, Equation (2) is presented as follows:

$$(\sigma_\gamma + d\sigma_\gamma)(r + dr)(t + dt)d\theta - \sigma_\gamma trd\theta - \mu p R_{tool}d\beta rd\theta = 0 \tag{4}$$

By ignoring the second-order differential terms, Equation (4) is simplified as follows:

$$d\sigma_\gamma r t + \sigma_\gamma r dt + \sigma_\gamma t dr - \mu p R_{tool} r d\beta = 0 \tag{5}$$

By using Equation (1) and substituting r in Equation (5), the following equation is obtained:

$$d\sigma_\gamma R_{tool} t \sin\beta + \sigma_\gamma R_{tool} \sin\beta dt + \sigma_\gamma R_{tool} t \cos\beta d\beta - \mu p R_{tool}^2 \sin\beta d\beta = 0 \tag{6}$$

Two sides of Equation (6) are distributed on this term; therefore,

$$\frac{d\sigma_Y}{dt} + \frac{\sigma_Y}{t} + \sigma_Y \cot\beta \frac{d\beta}{dt} - \frac{\mu p R_{tool}}{t} \frac{d\beta}{dt} = 0 \quad (7)$$

Now, to simplify Equation (7), one of the variables of this differential equation should be removed. Therefore, by using trigonometric rules, an acceptable estimation of changes in sheet thickness during the forming process can be obtained

$$t = t_0 \sin\left(\frac{\pi}{2} - \beta\right) = t_0 \cos\beta \quad (8)$$

By taking the derivative of two sides of Equation (8), $\left(\frac{d\beta}{dt}\right)$ is calculated as follows:

$$dt = -t_0 \sin\beta d\beta \Rightarrow \frac{d\beta}{dt} = -\frac{1}{t_0 \sin\beta} \quad (9)$$

In Equation (9), the negative sign indicates that the sheet thickness is reduced from point B to point A, by increasing the angle β . By using Equations (8) and (9), differential Equation (7) can be simplified as follows:

$$\frac{d\sigma_Y}{-t_0 \sin\beta d\beta} + \frac{\sigma_Y}{t_0 \cos\beta} + \sigma_Y \cot\beta \left(-\frac{1}{t_0 \sin\beta}\right) - \frac{\mu p R_{tool}}{t_0 \cos\beta} \left(-\frac{1}{t_0 \sin\beta}\right) = 0 \quad (10)$$

Hence:

$$\frac{d\sigma_Y}{d\beta} - \sigma_Y \tan\beta + \sigma_Y \cot\beta - \frac{\mu p R_{tool}}{t_0 \cos\beta} = 0 \quad (11)$$

By considering the incremental forming process as a straining process and by using constant volume law in the plastic area, the main strain equation is obtained as follows:

$$d\varepsilon_\theta = 0, d\varepsilon_Y + d\varepsilon_\theta + d\varepsilon_n = 0 \Rightarrow d\varepsilon_Y = -d\varepsilon_n \quad (12)$$

By using flow law, a relationship between stress and strain values in the plastic region can be found. Thus, one of the stress parameters can be calculated as the function of the two other parameters:

$$\frac{d\varepsilon_Y - d\varepsilon_\theta}{\sigma_Y - \sigma_\theta} = \frac{d\varepsilon_\theta - d\varepsilon_n}{\sigma_\theta - \sigma_n} \Rightarrow \frac{d\varepsilon_Y}{\sigma_Y - \sigma_\theta} = \frac{d\varepsilon_Y}{\sigma_\theta - \sigma_n} \Rightarrow \sigma_\theta = \frac{1}{2}(\sigma_Y + \sigma_n) \quad (13)$$

According to von Mises equation, the relationship between the main stress and yield stress is defined as follows:

$$Y = \frac{1}{\sqrt{2}} \sqrt{\left(\sigma_Y - \frac{1}{2}(\sigma_Y + \sigma_n)\right)^2 + \left(\frac{1}{2}(\sigma_Y + \sigma_n) - \sigma_n\right)^2 + (\sigma_n - \sigma_Y)^2} \quad (14)$$

By using Equation (13) and substituting σ_θ in von Mises equation, the following equation is obtained:

$$Y = \frac{\sqrt{3}}{2} |\sigma_Y - \sigma_n| \Rightarrow Y = \frac{\sqrt{3}}{2} |\sigma_Y + p| \Rightarrow \boxed{p = \frac{2\sqrt{3}}{3} Y - \sigma_Y} \quad (15)$$

By using the above equation, Equation (11) is simplified as follows:

$$\frac{d\sigma_Y}{d\beta} - \sigma_Y \tan\beta + \sigma_Y \cot\beta - \frac{\mu \left(\frac{2\sqrt{3}}{3} Y - \sigma_Y\right) R_{tool}}{t_0 \cos\beta} = 0 \quad (16)$$

The above differential equation can be presented as follows:

$$\frac{d\sigma_Y}{d\beta} + \sigma_Y \left(\cot\beta - \tan\beta - \frac{\mu R_{tool}}{t_0 \cos\beta}\right) - \frac{2\sqrt{3}}{3} \frac{\mu Y R_{tool}}{t_0 \cos\beta} = 0 \quad (17)$$

Two sides of Equation (17) are multiplied by the integrator factor $\left(K(\beta) = \left(\frac{\cos\beta}{1+\sin\beta}\right)^{\frac{\mu R_{tool}}{t_0}} \sin\beta \cos\beta\right)$; therefore,

$$d\left(\sigma_Y K(\beta)\right) = \frac{2\sqrt{3}}{3} \frac{\mu Y R_{tool}}{t_0 \cos\beta} K(\beta) d\beta \quad (18)$$

By integrating two sides of the above equation in $(0 \leq \beta \leq \alpha)$, the value of σ_Y is calculated as a function of α as follows:

$$\sigma_Y(\alpha) = \frac{2\sqrt{3}}{3} \frac{\mu Y R_{tool}}{t_0 K(\alpha)} \int_0^\alpha \frac{K(\beta)}{\cos\beta} d\beta \quad (19)$$

If the two terms M and $f(\alpha)$ are defined as follows:

$$M = \frac{\mu R_{tool}}{t_0} \quad (20)$$

$$f(\alpha) = \frac{1}{K(\alpha)} \int_0^\alpha \frac{K(\beta)}{\cos\beta} d\beta \quad (21)$$

then,

$$\sigma_Y = Y \left(\frac{2\sqrt{3}}{3} \frac{\mu R_{tool}}{t_0}\right) f(\alpha) \quad (22)$$

As shown, in Equation (20), the value of M depends on μ , R_{tool} and t_0 , which are the known parameters in experiments. However, due to the complexity of the function $k(\beta)$, the above integral is indeterminate and determining the value of stress along γ as a clear equation is not possible. When the value of M is as a coefficient of 0.5, a clear solution of this integral is available. In other cases, the largest approximation can be used or the value of integral can be obtained numerically. Additionally, in experimental tests, the radius of the forming tool is usually between 2.5 and 8 mm, the thickness of the metal sheet is almost 0.8 to 3 mm, and if the friction coefficient between surfaces is almost 0.1 to 0.25, the amount of M is between 0.5 and 2. It should be noted that by slightly changing these three parameters, the above-mentioned assumption is valid. These equations were solved for $M=1$ by Saberi et al. [32], and in this research, the equations are derived for other values of M.

The purpose of this research is to obtain a simple analytical equation for estimating the values of stress and force in this process, while, after integrating, these equations become more complex; hence, an equation with the function $f(\alpha) = \frac{A}{\cos^2 \alpha} + C$ is fitted in equations for different values of M . The values of A and C corresponding to the values of M are presented in Table 1. According to the values of R^2 , the accuracy of the coincidence of fitted equations is acceptable.

By using Equation (23), stress along γ is calculated.

$$\sigma_\gamma = \frac{2\sqrt{3}}{3} Y \left(\frac{\mu R_{\text{tool}}}{t_0} \right) \left(\frac{A}{\cos^2 \alpha} + C \right) \quad (23)$$

After calculating stress along γ , the value of normal stress is determined by Equation (15). By neglecting small values of tangential and normal stress, the vertical force applied by the tool to the metal sheet is obtained by Equation (24):

$$(dF_{\text{tool}})_n = \text{pr}d\theta R_{\text{tool}} d\beta \quad (24)$$

Using Equations (1) and (15) and integrating the two sides of the above equation, the following equation is obtained:

$$(F_{\text{tool}})_n = R_{\text{tool}} \int_0^\pi \left(\int_0^\alpha \text{pr}d\beta \right) d\theta = \frac{\pi R_{\text{tool}}}{2} \int_0^\alpha \left(\frac{2\sqrt{3}}{3} Y - \sigma_\gamma(\beta) \right) (R_{\text{tool}} \sin\beta) d\beta \quad (25)$$

In Equation (25), the contact of the tool with the sheet along peripheral direction equals $\frac{\pi}{2}$, in radians. Now, the value of vertical force applied to the spherical-head tool can be calculated based on Equation (26):

$$(F_{\text{tool}})_n = \frac{\pi}{2} Y R_{\text{tool}}^2 \times \int_0^\alpha \left(\frac{2\sqrt{3}}{3} - \frac{2\sqrt{3}}{3} (M) \left(\frac{A}{\cos^2 \beta} + C \right) \right) \sin\beta d\beta \quad (26)$$

In most studies, the applied vertical force along the vertical direction to the tool is obtained. To calculate this force, Equation (27) is used:

$$(F_{\text{tool}})_{ny} = (F_{\text{tool}})_n \cos\alpha = \frac{\sqrt{3}}{3} \pi Y R_{\text{tool}}^2 \cos\alpha \times \left((1 - \cos\alpha) + M \left(A + C \cos\alpha - \frac{A}{\cos\alpha} - C \right) \right) \quad (27)$$

TABLE 1. Values of A and C corresponding to the values of M

M	A	C	R^2
0.5	0.2135	0.5012	0.9903
1	0.1204	0.3126	0.9965
1.5	0.0913	0.1005	0.9903
2	0.3122	-0.6980	0.9917

3. EXPERIMENTAL TESTS

The required equipment and their arrangement in TPIF are shown in Figure 7. By using this equipment and a CNC, the forming process can be performed.

The mold has two separate parts. The first part, on which the guides are placed, is fixed on the milling machine table. In this part, the punch is located and stabilized at the bottom of the sheet between the guides of mold (the fixed part), and the punch is set on it with some bolts. The second part of the mold (the movable part) is placed inside the guides and cannot be displaced along the vertical direction. This part of the mold, where the sheet and the clamp are placed and the two sheets are locked between them, can be detached from guides and separated from the fixed part. In this research, the tools are spherical-head cylinders with different diameters made by MO40 steel as shown in Figure 8.

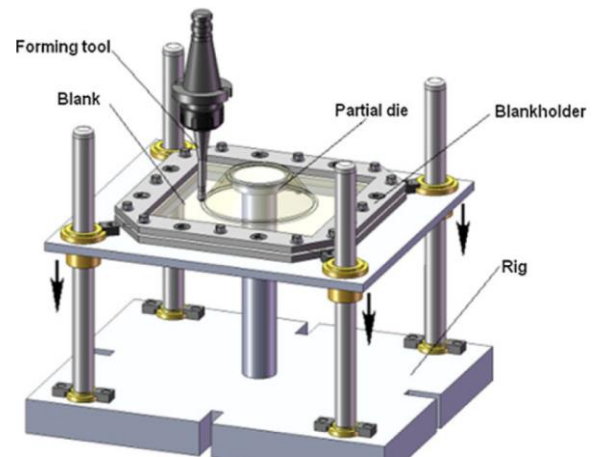


Figure 7. Experimental setup for two-point incremental forming [28]



Figure 8. Cylindrical tools with diameters of 5, 8, 12 and 16 mm

In Figure 9, the equipment used for the TPIF process of the present research is shown.

In the TPIF process, the punch creates a three-dimensional geometry for guiding the sheet and being a constant support for placing the sheet, and finally creating the form of punch on the sheet. Since in the TPIF method, compared to conventional forming techniques, forming forces are weak, there is no need for manufacturing the punch from solid materials. Since it is possible in the present study to cast pure blocks and proper machining, the punch is made of aluminum.

In the present research, a dynamometer is used to measure forces in incremental forming of the sheet on a CNC. The dynamometer is a KISTLER 9257B installed at the bottom of a mold supporting the metal sheet on the CNC table as shown in Figure 9. The direction of the z-axis of the dynamometer is along the axis of the incremental forming tool. Furthermore, the X and Y axes of the dynamometer are along X and Y directions of the CNC machine. In Figure 10, the incomplete pyramid formed by the TPIF process is shown.

4. RESULTS AND DISCUSSION

To investigate the validity of equations and to calculate the direction of the tool force in TPIF, a series of



Figure 9. Equipment used in TPIF process

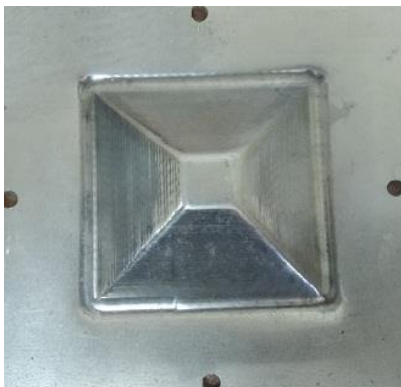


Figure 10. Incomplete pyramid formed by TPIF process

experimental tests are carried out, and important parameters of these tests are presented in Table 2. Using numerical simulation, the coefficient of friction between tool and sheet is determined [33].

First, the conditions in Table 2 and Equation (27) are used to plot the force graphs for different values of M (Figure 11). Experimental tests are performed at an angle of 55° ; hence, in Figure 11, the intersection of force graphs for different values of M at an angle of 55° is specified with a vertical line.

In experimental tests, the values of force are measured using a dynamometer for the conditions mentioned in Table 2 and a pyramid with an angle of 55° and two tools with diameters of 8 and 16 mm. The curves of the forces applied to the corresponding tools are shown in Figure 12. These curves have been plotted using the Dynoware software, which is specific to the employed dynamometer.

The values of M proportional to each tool and the values obtained for tool force from Equation (27) are presented in Figure 11, and the average values of force obtained from experimental tests are depicted in Figure 12 and presented in Table 3. In the experimental tests, the values of force are obtained by the dynamometer and the average is calculated with the accompanying software.

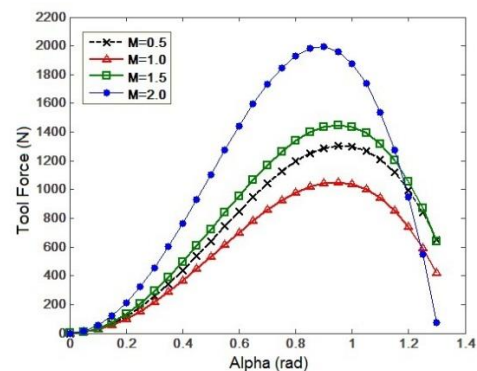


Figure 11. Force curves based on equation (27) for different values of M

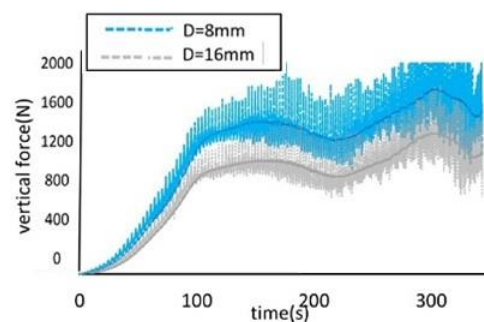


Figure 12. Vertical forces applied to tools with diameters of 8 and 16 mm for a pyramid angle of 55°

TABLE 2. Important parameters in experimental tests

Coefficient of friction between tool and sheet	Initial dimensions of sheet	Tool diameter	Sheet thickness	Sheet material	Yield stress of sheet
0.15	1800×1800 mm ²	8, 16 mm	1.2 mm	Aluminum 5053	210 MPa

TABLE 3. M values proportional to each tool and corresponding forces

Tool diameter (mm)	Friction coefficient	Sheet thickness	M value	Force (Equation (27))	Average force (experimental tests)
8	0.15	1.2	0.5	1300	1360
16	0.15	1.2	1	1050	1080

According to the values presented in Table 3 and the comparison of the forces calculated from Equation (27) and experimental tests, it can be seen that the maximum calculated error is 5%; that is, the results are in good agreement and the accuracy of equations is confirmed.

5. CONCLUSION

According to Figure 11, by increasing the angle α , the force applied to the tool enhances and the local strain created toward down side increases; based on $t=t_0\cos\alpha$, the change in the sheet thickness also increases. Hence, the enhancement of force with an increase in α is logical. The other point observed in Figure 11 is that at larger angles, the tool force is reduced. By increasing the angle of the punch wall, due to the reduction in contact between the surface of the tool, less compressive stress is applied to the metal sheet, and this is confirmed in Equations (15) and (23). Therefore, the force applied to tool with the enhancement of α increases, and at large angles, this force is reduced.

As shown in Equation (23), by decreasing the tool radius and increasing the sheet thickness, the stress created along γ is reduced. Therefore, due to the reduction in vertical stress, the sheet formability enhances. Ham and Jeswiet [34] confirmed the dependency of formability to tool radius and sheet thickness by using experimental tests.

One of the limitations of the incremental forming method is bearing the applied force by the machine during the process. In this research, an equation is presented for the prediction of the approximate value of the force applied to the tool. In this equation, with known values of the sheet yield stress, friction coefficient, tool radius and sheet thickness, the approximate value of the force applied to the tool can be calculated.

5. REFERENCES

- Naganathan, A., Penter, L., Sheet metal forming processes and applications, Hot stamping, ASM International, (2012).
- Edward, L., "Apparatus and process for incremental die less forming", Google Patents, (1967).
- Mason, B., Appleton, E., "Sheet metal forming for small batches using sacrificial tooling", Proceedings of the 3rd International Conference on Rotary Metalworking Processes, (1984), 495-512. doi : 10.1049/tpe.1984.0213 .
- Micari, F., Ambrogio, G., Filice, L., "Shape and dimensional accuracy in single point incremental forming: state of the art and future trends", *Journal of Materials Processing Technology*, Vol. 191, No. 1-3, (2007), 390-395. doi: 10.1016/j.jmatprotec.2007.03.066 .
- Filice, L., Ambrogio, G., Gaudio, M., "Optimized tool-path design to reduce thinning in incremental sheet forming process", *International Journal of Material Forming*, Vol. 6, No. 1, (2013), 173-178. doi: 10.1007/s12289-011-1065-4 .
- Tisza, M., "General overview of sheet incremental forming", *Journal of Achievements in Materials and Manufacturing Engineering*, Vol. 55, No. 1, (2012), 113-120.
- Attanasio, A., Ceretti, E., Giardini, C., Mazzoni, "Asymmetric two points incremental forming: improving surface quality and geometric accuracy by tool path optimization", *Journal of Materials Processing Technology*, Vol. 197, No. 1-3, (2008), 59-67. doi : 10.1016/j.jmatprotec.2007.05.053_.
- Duou, J., Callebaut, B., Verbert, J., De Baerdemaeker, "Laser assisted incremental forming: formability and accuracy improvement", *CIRP Annals-Manufacturing Technology*, Vol. 56, No. 1, (2007), 273-276. doi: 10.1016/j.cirp.2007.05.063 .
- Fan, G., Gao, L., Hussain, G., Wu, Z., "Electric hot incremental forming: a novel technique", *International Journal of Machine Tools and Manufacture*, Vol. 48, No. 15, (2008), 1688-1692. doi : 10.1016/j.ijmachtools.2008.07.010 .
- Ji, Y., Park, J., "Formability of magnesium AZ31 sheet in the incremental forming at warm temperature", *Journal of Materials Processing Technology*, Vol. 201, No. 1-3, (2008), 354-358. doi: 10.1016/j.jmatprotec.2007.11.206 .
- M. Ham and J. Jeswiet, "Single point incremental forming and forming criteria for AA3003", *CIRP Annals - Manufacturing Technology*, Vol. 55, No. 1, (2006), 241-244. doi : 10.1016/s0007-8506(07)60407-7 .
- Minutolo, FC., Durante, M., Formisano, A., Langella, A., "Evaluation of the maximum slope angle of simple geometries carried out by incremental forming process", *Journal of Materials Processing Technology*, Vol. 194, No. 1-3, (2007), 145-150. doi: 10.1016/j.jmatprotec.2007.04.109 .
- A. Bhattacharya, K. Maneesh, N. Venkata and J. Cao, "Formability and surface finish studies in single point incremental forming", *Journal of Manufacturing Science and Engineering*, Vol. 133, No. 6, (2011). doi: 10.1115/1.4005458 .

14. Ambrogio, G., Filice, L., Fratini, L., Micari, F., "Process mechanics analysis in single point incremental forming", *AIP Conference Proceedings*, Vol. 712, No. 1, (2004), 922-927. doi: 10.1063/1.1766645 .
15. Hussain, G., Gao, L. and Zhang, Z., "Formability evaluation of a pure titanium sheet in the cold incremental forming process", *The International Journal of Advanced Manufacturing Technology*, Vol. 37, No. 9, (2008), 920-926. doi: 10.1007/s00170-007-1043-7.
16. Nguyen, D., Park, J., Lee, H., Kim, Y., "Finite element method study of incremental sheet forming for complex shape and its improvement", *Proceedings of the Institution of Mechanical Engineers, Part B: Journal of Engineering Manufacture*, Vol. 224, No. 6, (2010), 913-924. doi: 10.1243/09544054jem1825 .
17. Han, F., Mo, J-h., "Numerical simulation and experimental investigation of incremental sheet forming process", *Journal of Central South University of Technology*, Vol. 15, No. 5, (2008), 581-587. doi: 10.1007/s11771-008-0109-5 .
18. Yamashita, M., Gotoh, M., Atsumi, S-Y., "Numerical simulation of incremental forming of sheet metal", *Journal of Materials Processing Technology*, Vol. 199, No. 1-3, (2008), 163-172. doi: 10.1016/j.jmatprotec.2007.07.037.
19. Zhou, LR., "Study on mechanism of NC sheet metal incremental forming", *Advanced Materials Research*, Vol. 239, (2011), 940-943. doi: 10.4028/www.scientific.net/amr.239-242.940 .
20. Shim, M.-S. and Park, J.-J., "The formability of aluminum sheet in incremental forming", *Journal of Materials Processing Technology*, Vol. 113, No. 1, (2001), 654-658. doi: 10.1016/s0924-0136(01)00679-3 .
21. Kim, Y. and Park, J., "Effect of process parameters on formability in incremental forming of sheet metal", *Journal of Materials Processing Technology*, Vol. 130, (2002), 42-46. doi: 10.1016/s0924-0136(02)00788-4.
22. Hirt, G., Ames, J., Bambach, M., Kopp, R., Forming strategies and process modelling for CNC incremental sheet forming. *CIRP Annals-Manufacturing Technology*, Vol. 53, No. 1, (2004), 203-206. doi: 10.1016/s0007-8506(07)60679-9 .
23. Silva, M., Nielsen, P., Bay, N., Martins, P., (2011). Failure mechanisms in single-point incremental forming of metals. *International Journal of Advanced Manufacturing Technology*, Vol. 56, No. 9, (2011), 893-903. doi: 10.1007/s00170-011-3254-1.
24. Seong, D.Y., Haque, M.Z., Kim, J.B., Stoughton, T.B. and Yoon, J. W., "Suppression of necking in incremental sheet forming", *International Journal of Solids and Structures*, Vol. 51, No. 15-16, (2014), 2840-2849. doi: 10.1016/j.ijsolstr.2014.04.007 .
25. Kurra, S. and Regalla, S. P., "Experimental and numerical studies on formability of extra-deep drawing steel in incremental sheet metal forming", *Journal of Materials Research and Technology*, Vol. 3, No. 2, (2014), 158-171. doi: 10.1016/j.jmrt.2014.03.009 .
26. Oraon, M., Sharma, V., Predicting Force in Single Point Incremental Forming by Using Artificial Neural Network. *International Journal of Engineering, Transaction A: Applications*, Vol. 31, No. 1, (2018), 88-95. doi: 10.5829/ije.2018.31.01a.13.
27. Silva, M., Skjoedt, M., Martins, P., Bay, N., (2008). Theory of single point incremental forming. *CIRP Annals Manufacturing Technology*, Vol. 57, No. 1, (2008), 247-252.
28. Emmens, W.C., Sebastiani, G. and van den Boogaard, A. H., "The technology of incremental sheet forming-a brief review of the history", *Journal of Materials Processing Technology*, Vol. 210, No. 8, (2010), 981-997. doi: 10.1016/j.jmatprotec.2010.02.014.
29. Perez-Santiago, R., Fiorentino, A., Marzi, R., Rodriguez, C., (2011). Advances in simulation of two point incremental forming. *AIP Conference Proceedings*, Vol. 1353, No. 1, (2011), 183-188. doi: 10.1063/1.3589512 .
30. Wang, QC., Hu, HH., Wu, JH., Cao, J., (2014). Research on Forming Accuracy of Two Point Incremental Forming for Aluminum 1060. *Advanced Materials Research*, Vol. 936, (2014), 1725-1729. doi: 10.4028/www.scientific.net/amr.936.1725 .
31. Saberi, A., Safavi, M., Kadkhodaei, M., Rabiei, F., Two-point incremental forming analysis using slab method and experimental data. *Modares Mechanical Engineering*, Vol. 13, No. 1, (2013), 61-69.
32. Silva, M. B., and Martins, P. A. F., "Two-Point Incremental Forming with Partial Die: Theory and Experimentation", *Journal of Materials Engineering and Performance*, Vol. 22, No. 4, (2013), 1018-1027. doi: 10.1007/s11665-012-0400-3 .
33. Esmailian, M., Khalili, Kh., "Finite element simulation of two-point incremental forming of free-form parts". *Iranian Journal of Materials Forming*, Vol. 5, No. 2, (2018), 26-35.
34. Ham, M., Jeswiet, J., "Forming Limit Curves in Single point incremental forming and the forming criteria for AA3003", *CIRP Annals-Manufacturing Technology*, Vol. 56, No. 1, (2010), 277-280. doi: 10.1016/j.cirp.2007.05.064.

Persian Abstract

چکیده

شکل‌دهی افزایشی مرحله‌ای دو نقطه‌ای یک روش جدید برای تولید قطعات پوسته‌ای با هندسه‌ی آزاد است. هدف اصلی این تحقیق به‌دست آوردن نیروی وارد به ابزار در فرایند شکل‌دهی افزایشی دو نقطه‌ای است. یکی از محدودیت‌های این فرایند، مقدار نیروی وارد بر ابزار است که دستگاه در حین فرایند می‌تواند تحمل کند. در این تحقیق یک معادله به‌منظور پیش‌بینی این مقدار نیرو ارائه می‌شود، که با در اختیار داشتن مقادیر تنش تسلیم ورق، ضریب اصطکاک، شعاع ابزار و ضخامت ورق، می‌توان این نیرو را محاسبه کرد. با افزایش زاویه‌ی شکل‌دهی، مقادیر کرنش موضعی ایجاد شده و نیروی وارد بر ابزار افزایش می‌یابد، اما با افزایش زاویه‌ی دیواره‌ی پانچ به دلیل کاهش سطح تکیه‌ی ابزار، تنش فشاری کمتری روی ورق فلزی وارد می‌شود. معادلات تحلیلی ارائه شده در این تحقیق با نتایج به‌دست آمده از آزمون‌های تجربی تایید شده است.
